

# Emplacement and composition of steep-sided domes on Venus

Ellen R. Stofan,<sup>1</sup> Steven W. Anderson,<sup>2</sup> David A. Crown,<sup>3</sup> and Jeffrey J. Plaut<sup>1</sup>

**Abstract.** Steep-sided domes on Venus have surface characteristics that can provide information on their emplacement, including relatively smooth upper surfaces, radial and polygonal fracture patterns, and pits. These characteristics indicate that domes have surface crusts which are relatively unbroken, have mobile interiors after emplacement, and preserve fractures from only late in their history in response to endogenous growth or sagging of the dome surface. We have calculated the time necessary to form a 12-cm-thick crust for basalt and rhyolite under current terrestrial and Venusian ambient conditions. A 12-cm-thick crust will form in all cases in < 10 hours. Although Venusian lava flows should develop a brittle carapace during emplacement, only late-stage brittle fractures are preserved at steep-sided domes. We favor an emplacement model where early-formed surface crusts are entrained or continually annealed as they deform to accommodate dome growth. Entrainment and annealing of fractures are not mutually exclusive processes and thus may both be at work during steep-sided dome emplacement. Our results are most consistent with basaltic compositions, as rhyolitic lavas would quickly form thick crusts which would break into large blocks that would be difficult to entrain or anneal. However, if Venus has undergone large temperature excursions in the past (producing ambient conditions of 800–1000 K [e.g., *Bullock and Grinspoon*, 1996, 1998]), rhyolitic lavas would be unable to form crusts at high surface temperatures and could produce domes with surface characteristics consistent with those of Venusian steep-sided domes.

## 1. Introduction

Magellan data have revealed that the surface of Venus is dominated by volcanic landforms, including extensive flow fields, sinuous channels, and a wide range of volcanic edifice types [*Saunders et al.*, 1991; *Head et al.*, 1991, 1992; *Guest et al.*, 1992]. Among the most distinctive edifices are steep-sided domes (Figure 1), whose morphology may indicate that evolved lava compositions have erupted on Venus [*Head et al.*, 1991; 1992; *Pavri et al.*, 1992]. These features were informally called “pancake” domes owing to their flat-topped, steep-sided appearance. *Pavri et al.* [1992] identified 145 steep-sided domes, with diameters from 7 to 94 km and heights from 60 m to over 4 km.

The circularity and steep sides of the domes were interpreted to indicate that high-viscosity lavas, perhaps rhyolitic in composition, formed these features either in a single eruptive event [*Guest et al.*, 1992; *Head et al.*, 1992] or episodically [*Fink et al.*, 1993]. *McKenzie et al.* [1992] calculated Newtonian viscosities on the basis of the shapes of seven domes on Venus and concluded that they consisted of rhyolitic lavas. Although the model they used is consistent with the measured dome profiles, it does not include the effects of a crust or account for the dynamics of the flow front, which are significant factors in the emplacement of lava flows and domes on Earth [*Blake*, 1990; *Iverson*, 1990; *Fink et al.*, 1993; *Kilburn*, 1993]. Also, the viscosities derived by *McKenzie et al.* [1992] are based on an unconstrained and probably unrealistically long timescale for emplacement (700–7000 years).

Other studies have shown that compositional determinations are nonunique when based on gross morphologic properties. *Sakimoto and Zuber* [1993, 1995] modeled domes as radial viscous gravity currents, with an assumed cooling-induced viscosity increase to include the effects of crystallinity and silica content on gross dome morphology. They found that a range of physical properties (i.e., initial viscosity and crystal content) corresponding to compositions from basaltic to rhyolitic could explain steep-sided dome morphology and favored basaltic compositions for the domes [*Sakimoto and Zuber*, 1995]. Analyses by *Bridges* [1997, 1997] noted similarities in dimensions and appearance between Venusian steep-sided domes and basaltic seamounts.

*Pavri et al.* [1992] described two models for steep-sided domes: a compositionally evolved magma model, in which the high dome viscosity is due to a silicic composition, and a basaltic bubble-enhancement model, where the high viscosity is due to extrusion of basaltic foam following vesiculation in the upper part of a magma chamber. *Bridges* [1997] modeled the effects of ambient conditions on the eruption of basalts and rhyolites on Venus and Earth and concluded that Venusian steep-sided domes are likely basaltic, although a rhyolitic composition could not be ruled out. In addition, parameters other than composition have been shown to control flow morphology [e.g., *Fink and Griffiths*, 1990; *Bridges and Fink*, 1992]. For example, the vesiculation of silicic lavas and the resultant density differences strongly influence the surface characteristics of terrestrial domes [*Fink and Manley*, 1987; *Anderson and Fink*, 1990; *Fink et al.*, 1992].

Previous efforts to model Venusian dome emplacement have focused on gross dome morphology. However, the distributions of vesicular and glassy textures on terrestrial dome and flow surfaces can be used to understand their physical properties, emplacement processes, and cooling histories [*Fink*, 1980a; *Fink*

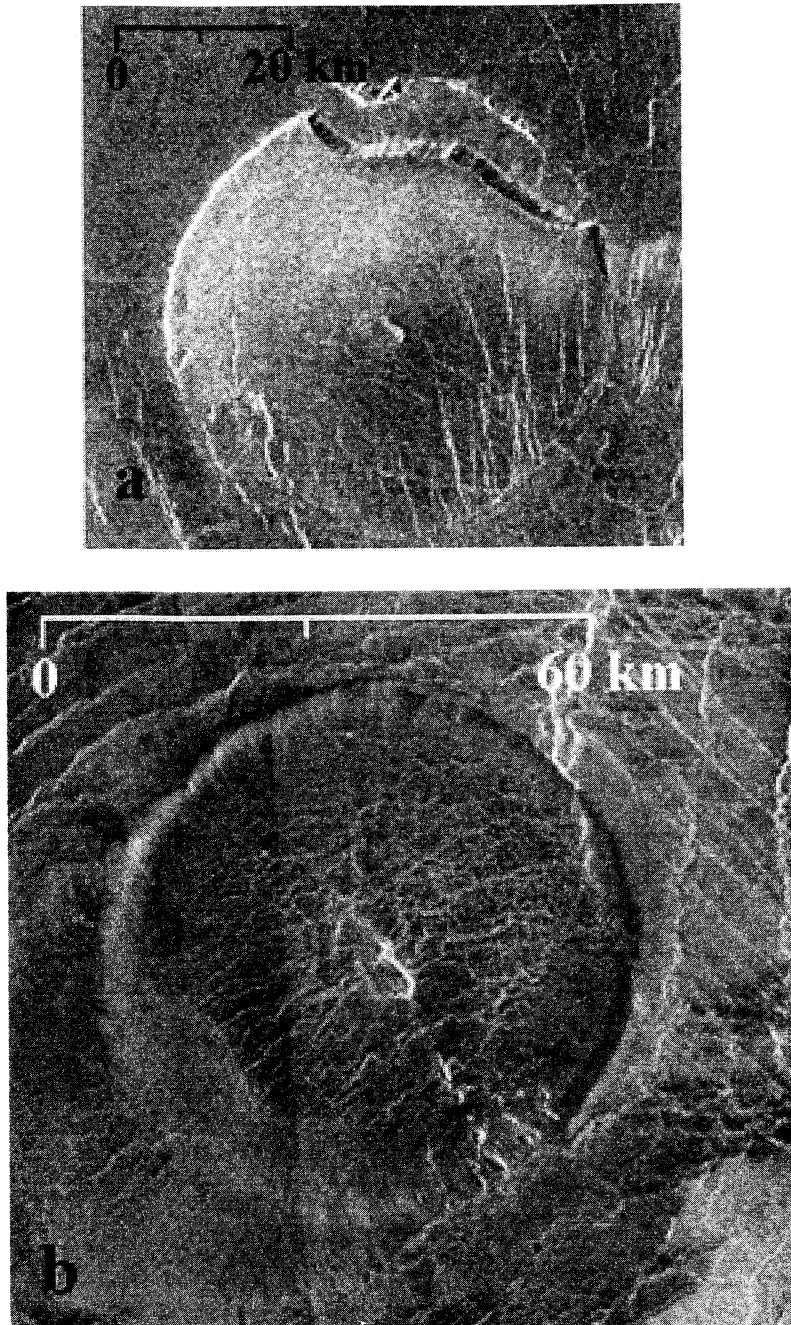


**Figure 1.** (a) Magellan radar image of a steep-sided dome located at  $34.0^{\circ}\text{N}$ ,  $311.2^{\circ}$  (P-40286, radar illumination from the left). The upper surface of the dome is relatively smooth, with a few pits. Fractures postdating dome emplacement cut the dome surface. (b) Magellan radar image of a steep-sided dome at  $12.6^{\circ}\text{N}$ ,  $8.2^{\circ}$  (C-MIDR 15N009, radar illumination from the left). Polygonal fractures cover much of the dome surface. Pits are seen at the center of the dome and along the southeastern margin. (c) Radial fractures extend from the central pit of this steep-sided dome. Note that the margins of the dome are rougher. This Magellan radar image is centered at  $2.9^{\circ}\text{S}$ ,  $150.9^{\circ}$  (F-MIDR 05S149, radar illumination from the left). The scale line above the dome is 40 km long. (d) Steep-sided dome with central polygonal fractures and marginal radial fractures. The dome also has two large central pits. The dome is centered at  $29.7^{\circ}\text{S}$ ,  $11.8^{\circ}$  in this Magellan radar image (F-MIDR 30S009, radar illumination from the left).

and Manley, 1987; Manley and Fink, 1987; Anderson and Fink, 1990]. In addition, the types, orientations, and distributions of surface features, such as ridges, fractures, creases, inflation structures, and blocks, provide constraints regarding the stress/strain histories of flow surfaces during emplacement

[Nichols, 1939; Fink and Fletcher, 1978; Fink, 1980a, 1980b, 1983, 1985; Fink and Manley, 1987; Sampson, 1987; Swanson *et al.*, 1987; Walker, 1991; Anderson and Fink, 1992; Rossi and Gudmundsson, 1996; Anderson *et al.*, 1998, 1999]. Steep-sided Venusian domes exhibit a variety of surface features [Johnson

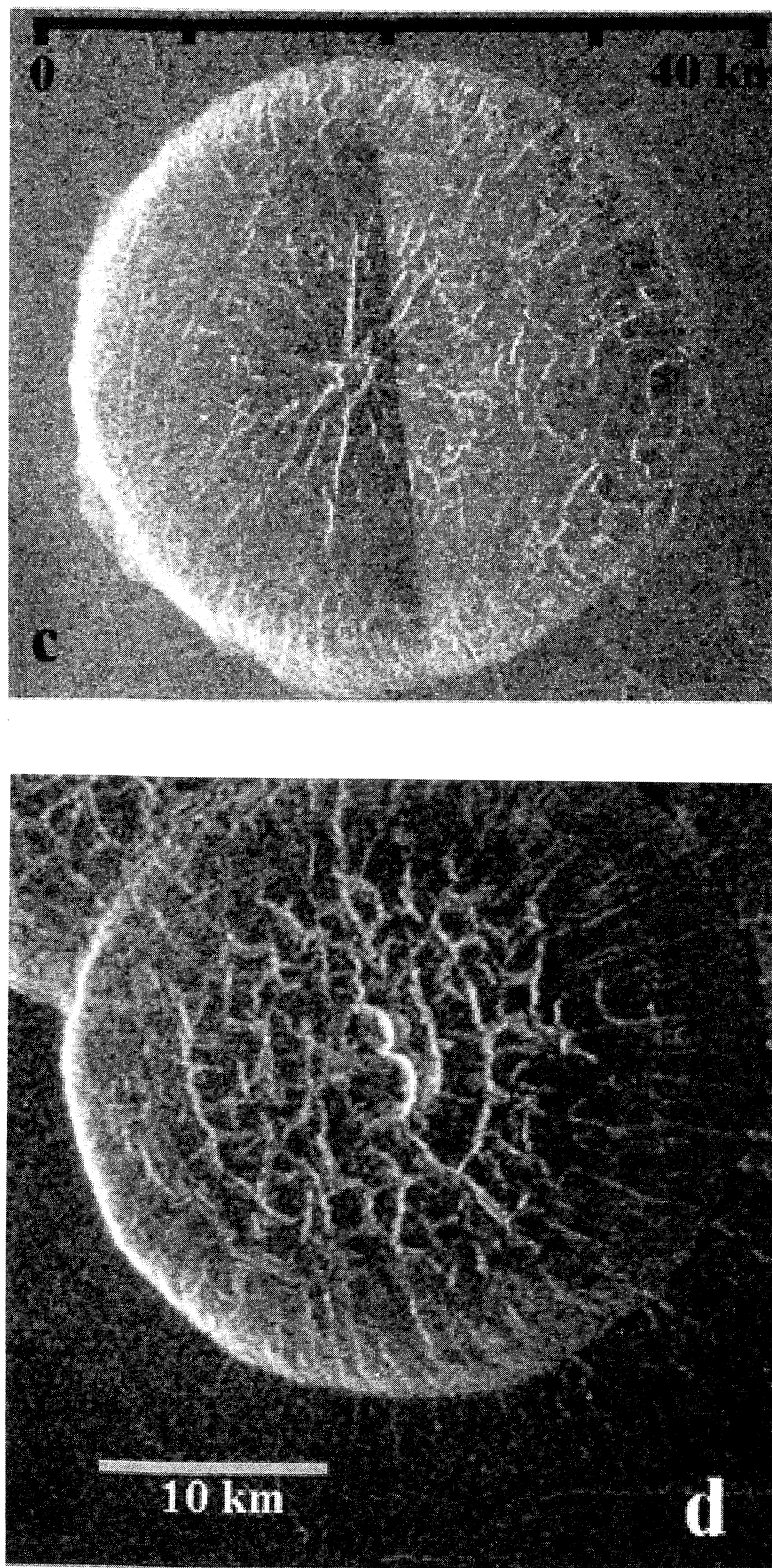


Figure 1. (continued)

and Sandwell, 1992; Pavri et al., 1992; Fink et al., 1993], permitting comparable analyses using Magellan data. We have compiled a database of morphologic and geologic characteristics of 175 large steep-sided domes, including location, size, geologic

setting, and surface characteristics (database available at [http://earth.agu.org/pubs/agu\\_elec.html](http://earth.agu.org/pubs/agu_elec.html)). Analyses of the physical attributes of the dome surfaces (i.e., surface roughness, fracture patterns, occurrence of pits) coupled with crustal growth

models are used to constrain emplacement processes for steep-sided domes. Our analysis supports a model involving emplacement of a low-viscosity fluid enclosed by an annealing crust that provides strength and controls dome planform. Our modeling suggests that basaltic compositions are most consistent with dome characteristics, although rhyolitic compositions emplaced under ambient conditions 200 K hotter than today (M. A. Bullock and D. H. Grinspoon, The recent evolution of climate on Venus, submitted to *Icarus*, 2000 (hereinafter referred to as Bullock and Grinspoon, submitted manuscript, 2000)) could also produce similar morphologies.

## 2. Surface Characteristics of Steep-Sided Domes

In order to provide detailed documentation of the physical attributes of steep-sided domes, we used Magellan Compressed-Once Mosaicked Image Data Records (C1-MIDRs) (225 m pixels) to locate domes >20 km in diameter, and Magellan (Full-Resolution Mosaicked Image Data Records (F-MIDRs) (75 m pixels) and (Full-Resolution Radar Mosaics (FMAPs) to study their surface characteristics and create a database of dimensions and morphologic characteristics. The image data from Magellan have an along-track resolution of 110 m and a cross-track ground resolution which varies from 101 to 250 m depending on latitude; the image data have been resampled at a pixel spacing of 75 m [Saunders *et al.*, 1992]. At the incidence angles of the Magellan radar the backscattered signal is dominated by surface roughness on the scale of the radar wavelength (12.6 cm). The altimeter footprint varied with latitude, with the highest-resolution data having a footprint of 1.9 km along-track and 12 km cross-track [Ford and Pettengill, 1992]. The effective range resolution of the altimeter is 88 m [Ford and Pettengill, 1992]. Roughness and reflectivity data are derived from the altimetry data.

We found 175 steep-sided domes with diameters from 19 to 94 km. This is a larger population of domes than catalogued by Pavri *et al.* [1992] owing to the inclusion of data from Magellan mapping cycles 2 and 3. Although we recognized steep-sided domes as small as 1-2 km, we restricted our detailed study to the larger domes listed in the database in order to reliably identify and analyze the distributions of surface structures. Features transitional between steep-sided domes and shields or cones were also found in the Magellan data but were not included in the database.

### 2.1. Gross Morphology and Geologic Setting

The majority of domes in the database are circular in plan view with distinct margins. Typically, domes appear to be flat-topped or concave, consistent with the findings of Pavri *et al.* [1992]. Domes studied with Magellan stereo data exhibit widely disparate profiles resulting from variations in margin steepness and summit irregularities [Plaut *et al.*, 1993, 1994]. Most dome surfaces have intermediate to low radar backscatter, have few surface fractures, and exhibit pits.

Elongate or irregular domes make up <10% of this survey; some of the irregular domes overlap with other steep-sided domes. Five domes had smaller domes completely superposed on them. Some steep-sided domes have scalloped margins, and a small number (nine) have slumps or flows extending from them [Guest *et al.*, 1992; Bulmer and Guest, 1996]. Two domes were identified with raised, rougher central regions interpreted to be vent complexes.

Nearly all of the domes occur near (within ~150 km) features of volcanic origin, as discussed by Pavri *et al.* [1992]. Forty-five percent of the domes in this survey are proximal to or within coronae. Another 43% occur in association with other volcanic features, including calderas, shields, and/or cones. Thirty-eight percent of domes are in chains of steep-sided domes; the largest chain has seven domes. Terrestrial volcanic domes also typically form in chains along a dike or fault [Fink and Pollard, 1983; Fink, 1985; Fink and Manley, 1987; Sampson, 1987; Scott, 1987; Reches and Fink, 1988]. Only three domes in this survey are isolated features in the plains. Over half (100) of all domes contain structures with orientations similar to those in the surrounding plains; some features extend from the plains into domes. The margins and/or interiors of some domes (12) appear to be highly degraded by burial, fracturing, and collapse [e.g., Guest *et al.*, 1992; Pavri *et al.*, 1992; Crown *et al.*, 1993]. One dome was identified that was clearly embayed by surrounding plains material, but in general, stratigraphic relations between domes and their surrounding units are difficult to determine.

### 2.2. Radar Properties

Most of the Venusian domes are located at midlatitudes, where the backscatter signal strength in Magellan data is dominated by surface features (e.g., rocks, cracks, undulations) comparable in scale to the 12.6-cm wavelength of the radar instrument. Ford [1994] derived backscatter values for 20 domes that were within 2 dB of the Venus average backscatter value, indicating that the backscatter of the plains and domes are essentially identical, given the calibration error budget of the data for the plains and for the domes. J.J. Plaut *et al.* (manuscript in preparation, 2000) measured the backscatter values at two incidence angles of four typical Venusian domes and also found that they did not differ significantly from the average backscatter for Venus, which is dominated by smooth plains surfaces. The specific backscatter cross section and scattering laws for the Venusian domes and plains (-10 to -20 dB at incidence angles of 25°-45°) are comparable to Hawaiian smooth pahoehoe and lava pond surfaces (J.J. Plaut *et al.*, manuscript in preparation, 2000). Domes in the survey of Pavri *et al.* [1992] have an altimeter-derived average rms slope of ~3°; moderately rough terrestrial pahoehoe flows on Kilauea Volcano have meter-scale rms slopes of 5°-12° [Campbell and Shephard, 1996], and terrestrial silicic domes have meter-scale rms slopes of 12°-43° (J.J. Plaut *et al.*, manuscript in preparation, 2000).

### 2.3. Pits

Three types of pit features are observed on steep-sided domes: (1) centrally located pits that may have concentric fractures (Figure 2a); (2) multiple pits scattered across dome surfaces or concentrated near dome margins (Figure 2b); and (3) pits with prominent raised rims that may occur in various locations on dome surfaces (Figure 2c). Eighty-one percent of the domes in this survey have at least one pit. Approximately 14% of the domes have a deep, smooth-floored central pit with a diameter >50% of the dome diameter (Figure 2c). Pit diameters range from the limits of resolution of the radar data to over 20 km. Pit depths for a subsample of the database were derived using manual stereo matching [Plaut, 1993], and range from tens of meters to nearly 1 km. These depths ranged from about 12 to 55% of the dome height.

On Earth, silicic domes also exhibit craters or pits. Mono Craters, a chain of rhyolite domes in eastern California, include

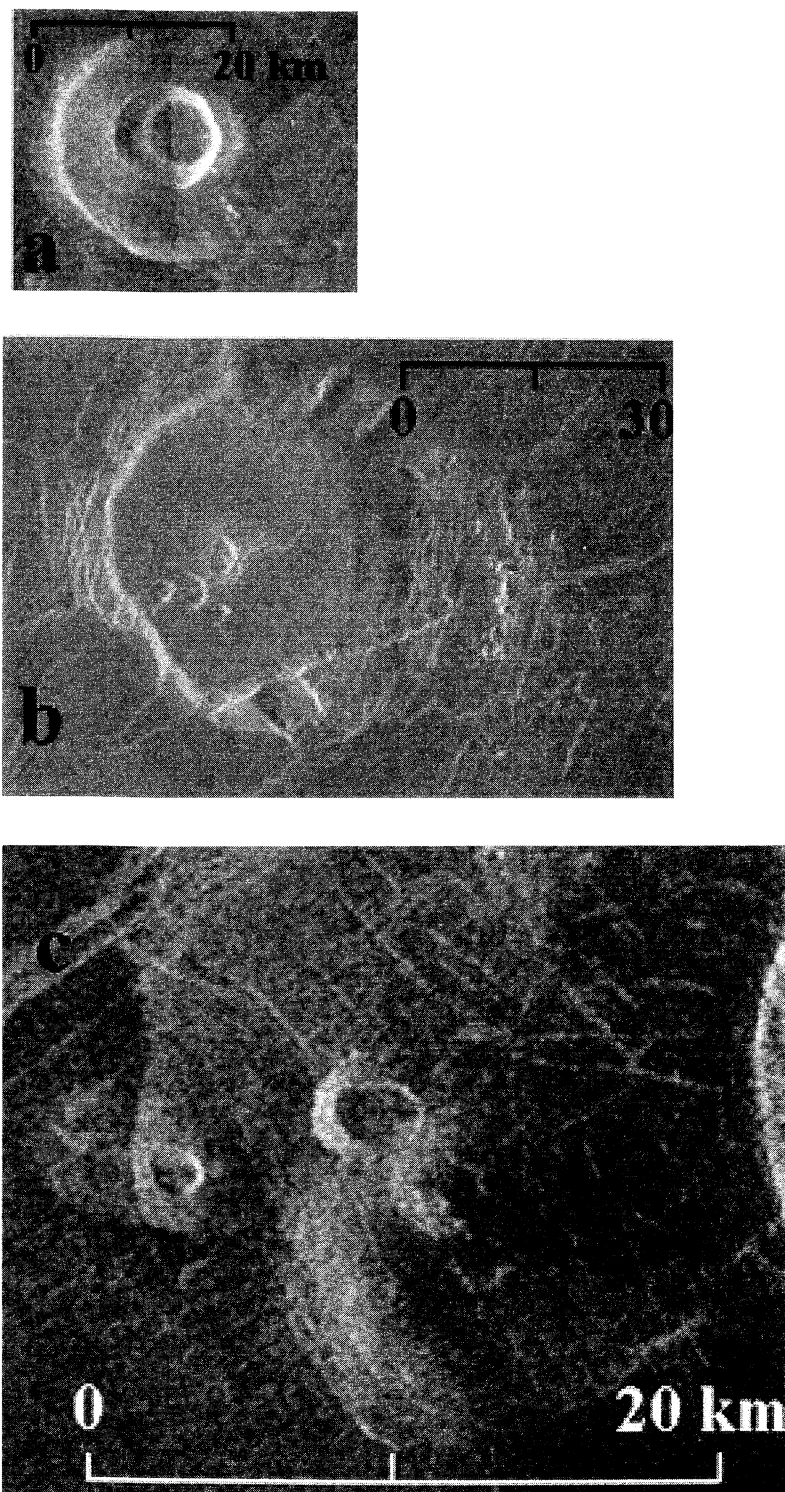


**Figure 2.** (a) Magellan radar image of steep-sided dome located at  $13.9^{\circ}\text{S}$ ,  $252.3^{\circ}$  (F-MIDR 15S254, radar illumination from the left). The central pit is over 10 km across, about half the diameter of the dome. (b) Steep-sided dome with partially scalloped margins, with scattered pits. This Magellan radar image is centered at  $33.7^{\circ}\text{N}$ ,  $311.8^{\circ}$  (P-40286, radar illumination from the left). (c) Magellan radar image of several overlapping steep-sided domes, centered at  $29.8^{\circ}\text{S}$ ,  $11.4^{\circ}$  (F-MIDR 30S009, radar illumination from the left). The large pit in the center of the image has distinct raised rims.

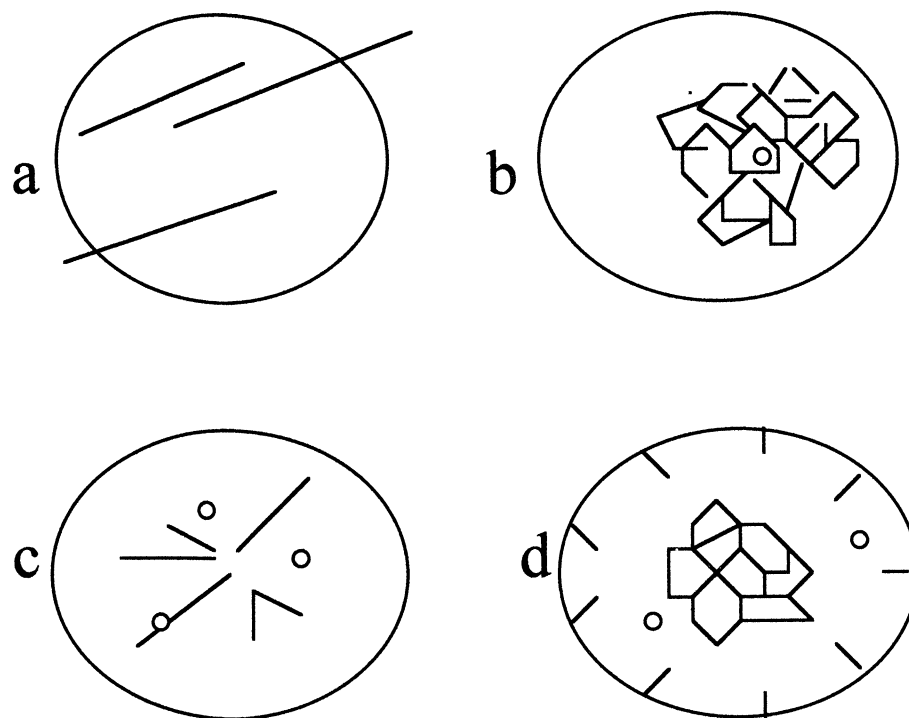


**Figure 3.** Diagram illustrating the different types of fractures on dome surfaces. (a) 57% of domes have throughgoing fractures; (b) polygonal fractures occur on 34% of domes; (c) 28% of domes have radial fractures; and (d) 7% of domes have both polygonal and radial fractures.

features with large (relative to dome diameter), centrally located, circular to elliptical summit craters [Smith, 1973]. These craters form by a combination of explosion and collapse of the rough, upper surface of a dome and in some cases can produce cratered domes within the summit crater of a preexisting dome. For comparison to the Venusian domes, one of the domes within the Mono chain is 365 m in diameter and has a summit depression 180 m wide and 46 m deep with a 70 x 35 m inner crater of 20-m depth. The larger, more shallow crater formed by subsidence, and the smaller, deeper crater formed by explosion [Smith, 1973]. The surfaces of rhyolite domes can also exhibit clusters of small pits 10-15 m deep which form owing to explosion of internal gas-rich zones near flow margins; these explosions can emplace small amounts of blocks and ash on the adjacent flow surface [Fink and Manley, 1987; Manley and Fink, 1987]. All of these examples of pits on terrestrial domes formed after emplacement of the dome, and primarily by explosions.

The formation of a surface pit requires the presence of a brittle crust. Pits on steep-sided domes are seen to both predate and postdate fractures, or occur isolated from fractures on the dome surfaces, indicating that pit and fracture formation overlapped in time and that all pits are not structurally controlled. Depths of the pits may reflect the minimum crustal thickness at the time of their formation; alternatively, pits may be purely postemplacement collapse features above subsurface voids, similar to Hawaiian pit craters [Walker, 1988].

#### 2.4. Fractures

Fractures on dome surfaces occur in radial, concentric, or polygonal patterns (Figure 1 and 3). Seventeen percent (30) of the steep-sided domes analyzed have no discernible surface

fractures, and another 29% (50) only have fractures that mimic regional deformation patterns (Figure 1a), indicating that nearly half of all large steep-sided domes have no resolvable surface fractures associated with their emplacement. Of the 175 domes surveyed, 34% (59) have polygonal fractures, 28% (49) have radial fractures, and 2% (four) have concentric features. Approximately one quarter of the radially fractured domes have radial fractures only at their margins. Most concentric features are also concentrated near the dome margins. We interpret most of the unresolvable concentric features as fractures because they lack the sinuosity characteristic of ridges. No distinct ridges have been identified on any of the steep-sided domes in this survey.

Polygons on dome surfaces are defined by intersecting fractures and range in size from several kilometers across down to the limit of resolution of the radar images (~120 m) (Figure 1b). Polygons are typically 1-5 km across and tend to be consistent in size across a dome surface. The linear features that make up the polygons are commonly 1-2 pixels across (<150 m). Some polygonally fractured domes occur on polygonally fractured plains, indicating that this pattern may not always be related solely to dome emplacement. Curved T, T, and Y polygonal intersections can be identified on dome surfaces and are typical of shrinkage cracks on Earth [Aydin and DeGraff, 1988]. They are also seen on polygonally fractured plains on Venus [Johnson and Sandwell, 1992] as well as terrestrial lava lakes [Macdonald, 1962].

At some domes, fracture patterns cover the entire dome surface, whereas at other domes, fracture patterns are concentrated at the margins and/or at the center of the dome. Most domes contain a single fracture type, although six domes have polygonally fractured interiors with radially fractured margins (Figure 1d), and seven have centrally located polygonal

and radial fractures. Two domes have polygonal fractures near the center and concentric fractures at their margins, and one dome has both concentric and radial features. At some domes, fracture patterns cover the entire dome surface in a relatively organized fashion, whereas at other domes, fracture patterns are concentrated at the margins and/or at the center of the dome. Fifty-three percent of the domes (93) exhibit throughgoing fractures that postdate dome emplacement. A small number of domes are so heavily fractured by throughgoing fractures that no preexisting deformation patterns could be identified.

### 2.5. Constraints on Dome Emplacement From Surface Analysis

Relatively radar-smooth surfaces coupled with the characteristics and distributions of pits and fractures constrain the nature and timing of crust formation and provide insight into dome emplacement and cooling. The presence of pits and fractures indicates that a brittle crust formed on the dome surfaces. The relatively smooth upper surfaces of the majority of steep-sided domes (*J.J. Plaut et al.*, manuscript in preparation, 2000) indicate that they are not blocky and therefore consist of largely unfragmented crusts. Domes that display undeformed pits, display simple fracture patterns, and lack preserved flow structures presumably did not form an appreciable brittle crust until the final stages of their emplacement. Domes with no surface fractures other than postemplacement regional deformation (44% of domes studied) indicate that insufficient stresses were produced by either flow or cooling to significantly fracture the crust at a scale resolvable by the Magellan radar or that no brittle crust formed during emplacement.

No clear evidence of ductile deformation is preserved on the Venusian dome surfaces examined in this study. This is in contrast to observations of the surfaces of terrestrial silicic domes [*Fink*, 1980a, 1983; *Plaut et al.*, 1993; *Anderson et al.*, 1994, 1998], which commonly display prominent, regularly spaced compressional ridges. Ridged units within rhyolitic and dacitic domes at Medicine Lake Volcano in northern California and rhyolitic domes of the Inyo Chain of eastern California exhibit structures with wavelengths between 10 and 15 m and amplitudes of 1-5 m [*Anderson et al.*, 1994]; the Chao dacite flow in the Central Andes of Chile has ridges with heights of ~30 m spaced 50 m apart [*Guest and Sanchez*, 1969; *de Silva et al.*, 1988]. Two large Venusian flows with ridges have been identified [*Moore et al.*, 1992; *Gregg et al.*, 1998]; these flows are slightly larger in size (over 100 km across) than the largest steep-sided domes. Ridge spacings on these flows are <1 km. Ridges at spacings larger than the scale of the radar resolution (~100 m) should be detected in the Magellan radar images, if the vertical expression is more than a few meters (*J.J. Plaut et al.*, manuscript in preparation, 2000). The presence of numerous, smaller ridges on steep-sided dome surfaces is not consistent with their relatively smooth radar signatures (*J.J. Plaut et al.*, manuscript in preparation, 2000). The lack of ridges suggests that the domes did not have a consistent viscosity gradient (regularly decreasing viscosity with depth) over a sufficiently large areal extent [*Fink and Fletcher*, 1978; *Fink*, 1980b, 1983; *Gregg et al.*, 1998]. Alternatively, either a stable crust did not exist during flow or the crust was not subjected to sufficient strain to cause folding [*Gregg et al.*, 1998].

The presence of pits and the measured concave profiles of the upper surfaces of some steep-sided domes [*Plaut et al.*, 1994] suggest that, in many cases, domes contained a fluid, mobile core.

The majority of pits appear to have formed by collapse, as they lack rims or surrounding deposits. Collapse pits indicate that a solid crust developed while the flow interior was still mobile, although extrusion may have ceased. Collapse of a brittle crust may have occurred into a void created by migration of lava in a dome's interior. The few rimmed pits observed indicate that some secondary activity was responsible for construction upon the dome surface, again providing evidence for a mobile interior under a stable crust. Some rimmed pits may result from small-scale pyroclastic activity [see *Head and Wilson*, 1986] and may be analogous to terrestrial cinder or spatter cones.

The formation of surface fractures requires a brittle medium and strain sufficient to exceed the strength of the crust. Fracture patterns reflect the spatial and temporal evolution of the state of stress in the brittle crust; fractures may form both during and following flow emplacement and may result from thermal stresses and response to lava transport. The fracture patterns observed on Venusian steep-sided domes can be used to constrain emplacement processes and physical properties of the dome lavas. The concentric fracture patterns observed on steep-sided dome surfaces suggest accommodation of the strain resulting from loss of volume in the dome interior, perhaps due to lava draining back into the conduit system or volatile exsolution. As in the case of collapse pits, concentric fractures provide additional evidence that dome interiors were mobile. The occurrence of concentric and polygonal fractures on a given dome surface is similar to that observed on lava lakes that have experienced significant sagging [*Macdonald*, 1962].

Polygonal fracture patterns are indicative of isotropic tensional stress in two dimensions (plane strain). This stress regime may originate from cooling [e.g., *Spry*, 1962; *Ryan and Sammis*, 1978, 1981; *Long and Wood*, 1986; *DeGraff and Aydin*, 1987, 1993; *Aydin and DeGraff*, 1988] or from tension produced by either sagging or expansion of a crust. At Kilauea Iki in Hawaii, sagging has resulted in a polygonally fractured lava lake surface, the center of which now lies several meters below its margins. Polygonal surface fractures were also observed during the expansion of the October 1980 Mount St. Helens dome; a number of large, intersecting incandescent fractures were observed on the convex upward surface of the growing dome [*Moore et al.*, 1981]. Polygonal fracture patterns, which are identified on approximately one third of Venusian domes, indicate that a relatively isotropic stress field existed after the formation of a crust on the dome surface. Polygonally fractured plains are relatively common on Venus; *Johnson and Sandwell* [1992] explained these features by invoking thermoelastic stresses within the lithosphere associated with an increase in the heat flux at the base of the lithosphere. Individual Venusian domes are insufficiently thick to produce the small gradients necessary to produce large polygons through thermal stresses alone, although polygonally fractured domes lying in polygonally fractured plains may reflect strain in the lithosphere that occurred well after dome emplacement. The large sizes of the polygons on the Venusian domes coupled with generally flat to concave upper surfaces suggests that these fractures originate from tension produced by sagging, rather than cooling stresses or expansion.

Radial stress regimes and their associated fracture patterns may be produced by a pressurized circular element within a rigid plate [*Johnson*, 1961, 1968]. Thus the radial fracture patterns evident on the surfaces of some Venusian domes may have originated by the stress produced by continued expansion of the dome through extrusion of material from a centrally located vent after a brittle surface crust had formed. Domes with polygonally

fractured interiors and radially fractured margins may reflect marginal deformation resulting from earlier extrusion, with later sagging in the interior producing the polygonal fractures.

The relatively smooth dome surfaces and the characteristics of surface fractures and pits indicate that brittle crusts formed on eruptive timescales on Venusian domes but that the crusts did not form a rubbly, broken surface during emplacement. Although experimental modeling suggests that composite eruptions can form circular domes [Fink *et al.*, 1993], the simple fracture patterns, lack of blocks, simple shape, and lack of boundaries formed by the intersection of composite dome lobes strongly suggest a single episode of dome emplacement [e.g., Head *et al.*, 1992].

### 3. Crusts on Venusian Domes

#### 3.1. Influence of Cooling on Crust Development

From analysis of dome surface morphology we cannot deduce whether the lack of folded and highly fragmented crusts at Venusian steep-sided domes indicates that crusts form late (and are predominantly affected by isotropic stress conditions after spreading has essentially ceased) or that they form early but the surfaces deformed during transport are not preserved. However, it seems unlikely that a brittle crustal layer could form early and flow for up to tens of kilometers without developing a blocky surface and exhibiting flow features indicative of transport which would be recognizable in Magellan radar images. Crustal growth rate models for Venusian conditions [e.g., Gregg and Sakimoto, 1996; Bridges, 1997] may rule out late-stage crusts and therefore can provide critical constraints on the emplacement mechanisms of steep-sided domes. In addition, because rhyolitic and basaltic magmas have different physical properties, we may be able to gain insight into which composition is favored on the basis of surface observations and model constraints.

Lava flow surfaces may respond to applied stress in a ductile or brittle manner, depending on both the physical properties of the lava near the surface and the strain rate. Ductile behavior is favored when strain rates are low and/or when the temperature of the lava at the surface is greater than the glass transition temperature (at which an abrupt increase in viscosity up to  $>10^{12}$  Pa S can occur [Ryan and Sammis, 1981; Stevenson *et al.*, 1996]). Brittle behavior is favored when strain rates are high and/or when the surface temperature is below the glass transition temperature. Although the surfaces of most terrestrial subaerial lavas supercool and quench (drop below the glass transition temperature) when exposed to the atmosphere, deeper lava and lavas in hotter environments will not supercool. In this case, brittle behavior ensues as slower cooling material crystallizes at solidus temperatures.

Low-viscosity lava flows such as basalt are seen in the field to typically display a crystalline interior beneath a 1- to 3-cm-thick glassy carapace after cooling; the glassy carapace represents the supercooled crust that quenched as it passed below its glass transition temperature ( $\sim 1000$  K for basalt [Ryan and Sammis, 1981]) and the crystalline flow interior represents material that crystallized as it passed through solidus temperatures and released latent heat of fusion. Recent terrestrial rhyolite flows, however, have glassy rinds that may extend tens of meters into the flow interior [Loney, 1968; Fink, 1983; Fink and Manley, 1987; Anderson and Fink, 1992]. Some small glassy rhyolite flows show no crystallization in their interiors, whereas some of

the larger extrusions have crystalline regions only deep within the flow interior where temperatures remained hot for many years [Fink and Manley, 1987]. The disparity in the thicknesses of glassy rhyolitic and basaltic lava flow carapaces results in large part from the great difference in viscosity between the two compositions. Although a range of rates have been observed [e.g., Cashman, 1990, 1993; Cashman *et al.*, 1999], increased rates of ion migration in low-viscosity fluids allow for crystal growth rates that are typically several orders of magnitude higher in basalt ( $5 \times 10^{-8}$  to  $1 \times 10^{-7}$  cm/s for plagioclase [Crisp and Baloga, 1994]) than for more silicic compositions ( $1 \times 10^{-11}$  to  $1 \times 10^{-9}$  cm/s for plagioclase in dacite [Cashman, 1992]), reflecting the fact that rhyolites typically vitrify and basalts typically crystallize.

As fast cooling lava flow surfaces quench or as slow cooling ones crystallize, they will exhibit brittle behavior when stressed. This colder material forms a brittle mechanical crust. These brittle crusts have considerable effects on flowing lava, influencing both the morphology [Iverson, 1990] and eruption dynamics [Anderson and Fink, 1989, 1990; Anderson *et al.*, 1995]. Flows that have started to cool but have not yet quenched or crystallized will develop a layer of higher-viscosity fluid at the surface. This material will tend to behave in a ductile manner and may develop regularly spaced folds if compressed [Fink, 1980b]. This colder but not yet brittle material forms a ductile mechanical crust. Ductile mechanical crusts may also form as brittle surface crust is broken during flow and entrained back into the upper regions of the flow. Crisp and Baloga [1994] suggested that entrained material may significantly affect the rate of cooling of the flow surface and should also affect the viscosity of the near-surface material owing to the introduction of solid fragments. Ductile mechanical crusts may have tensile strengths up to seven orders of magnitude greater than the flow interior [Kilburn, 1993].

Lava flow surface morphology thus depends on the relative rates of crustal growth and destruction [Kilburn, 1993]. For example, Kilburn [1993] postulated that pahoehoe lavas have greater crustal restraint and thus less widespread disruption of the crust. When crustal disruption occurs, such as in the formation of aa and block-lava flows, the thickness of the thermal crust may influence the size of blocks found on the flow surface. Quickly emplaced aa flows typically have clinker in the 3- to 8-cm-size range, whereas more slowly emplaced andesite, dacite, and rhyolite flows may have individual blocks exceeding 5 m in diameter [Anderson *et al.*, 1998]. Anderson *et al.* [1998] found that silicic flows that were rapidly emplaced had smaller average block sizes than more slowly emplaced flows presumably owing to their thinner crusts and higher strain rates.

Numerous investigators have considered the cooling of a lava flow surface and identified processes that affect the rate of crustal growth [e.g., Head and Wilson, 1986; Crisp and Baloga, 1990; Kilburn and Lopes, 1991; Griffiths and Fink, 1992a, 1992b; Gregg and Greeley, 1993; Kilburn, 1993; Crisp *et al.*, 1994; Bridges, 1997]. Upon contact with a planetary atmosphere the surface of a lava flow will lose heat most efficiently through radiation, resulting in a rapid decrease in lava surface temperature. According to Kilburn [1993], times necessary for basaltic flow surfaces to chill via radiation range from 160 to 200 s [Crisp and Baloga, 1990; Kilburn and Lopes, 1991]. However, this approach ignores the effects of atmospheric convection on cooling, which may be important on planets such as Venus that have dense atmospheres, especially during this initial stage of crustal development. Crustal growth rates for basaltic lava flows

are predicted to be greater initially (up to ~10 hours) on Venus relative to Earth owing to enhanced cooling by atmospheric convection [Head and Wilson, 1986; Gregg and Greeley, 1993].

Recently, modeling studies by Bridges [1997] considered the cooling of both basaltic and rhyolitic lavas under ambient conditions appropriate for subaerial and subaqueous environments on Earth and for the surface of Venus. Upon contact with the Venusian atmosphere, radiative and convective heat losses cause rapid cooling of the upper flow surface. Crystallization is minimal, and thus latent heat is not released during the formation of the glassy outer rind. Bridges [1997] estimated the time necessary to chill basaltic and rhyolitic lava flow surfaces to a brittle, glassy state (as defined by the glass transition temperature) for Venusian and subaerial conditions, with values of 100 s and 14 s for subaerial basalt and rhyolite, respectively, and 75 s and 13 s for the Venusian counterparts. Bridges [1997] also noted that variations in lava density (a function of composition and porosity) minimally affect the rates of cooling.

Heat transfer within a flow occurs by conduction beneath and through the cooled and thickening glassy rind. As cooling proceeds, the overall cooling rate is strongly influenced by the amount of heat released through crystallization of the magma. For times <1000 s, Bridges [1997] used the approach of Griffiths and Fink [1992b], in which latent heat is not considered during chilling of the upper surface, to model the initial growth of the crust. For times >10,000 s, Bridges [1997] assumed full crystallization and latent heat release and modeled crustal growth using the heat conduction equation (as done by Turcotte and Schubert [1982, p. 169]). Between 1000 and 10,000 s, Bridges [1997] assumed an increasing effect of latent heat on the cooling rate and manually connected the <1000 s and >10,000 s crustal thickness versus time curves through the 1000-10,000 s interval to schematically represent the transition from the production of a glassy crust to that of a crystal-rich crust.

Although the time available for crystallization controls how much latent heat is evolved, so do composition and crystallization/nucleation rates, as evidenced by subaerial basaltic flows with centimeter-scale glassy crusts and rhyolitic flows with glass extending tens of meters into the flow. Crisp et al. [1994] found rapid crystallization in active Mauna Loa basalt flows, where the volume percent of crystals increased from <10% to >30% within a few hours. Cashman and Taggart [1981] measured extremely small crystal growth rates of  $1 \times 10^{-9}$  cm/s in more silicic Mount St. Helens dacite. Thus, while crystal growth rates can vary, we suggest that the typical differences in basaltic and rhyolitic lava flows require different approaches in the treatment of the effect of crystallization on the cooling rate once the glassy surface rind is established through initial radiative and

convective heat loss. We also suggest that differences in cooling styles between basalt and rhyolite typically seen on Earth have implications for the brittle behavior of these two compositions; fully crystallizing basalts should become brittle at solidus temperatures in the absence of meteoritic water, whereas quenching, glassy rhyolite flows will exhibit brittle behavior as the material passes through the glass transition temperature.

### 3.2. Model of Crustal Formation

In order to incorporate differences in crystallization history for typical basalts and rhyolites to assess the nature and timing of potential brittle deformation, we have modeled the growth of a surface crust under terrestrial and Venusian conditions. As shown by Bridges [1997], the time required to form a glassy upper layer is nearly identical on Earth and Venus for the same composition and less than an order of magnitude different for basaltic and rhyolitic compositions. In fact, Bridges [1997] shows <1 cm difference in glassy rind thickness between subaerial basalt and Venusian rhyolite after 1000 s of cooling. We assume that terrestrial and Venusian basaltic and rhyolitic flows develop a thin glassy rind underlain by lava near the eruption temperature within the first 100 s of cooling. For basaltic compositions, release of latent heat is considered during subsequent cooling but ignored during the cooling of rhyolite flows. Although this approach does not include variations in cooling rate during the transition from glass formation to full crystallization in basalt flows, we find this approach preferable to the approach of Bridges [1997] because it (1) considers the difference in crystallization rates between basalts and rhyolites, (2) considers the differences in temperatures where brittle behavior is exhibited for lavas of different composition, and (3) does not require schematic representations of the transition between two disparate cooling curves. Although a range of glass transition temperatures have been reported for rhyolites [Murase and McBirney, 1970; Ryan and Sammis, 1981; Westrich et al., 1988; Neuville et al., 1993; Stevenson et al., 1996; Webb, 1997], we have chosen to use the Westrich et al. [1988] value of 943 K (Table 1), as it is within the reported range of values. We have also assumed that the temperature of the surface glassy rind remains 100 K above the ambient temperature throughout the time period over which we model conductive cooling. Although the surface temperature cools with time, this simple approach is consistent with observations that terrestrial flow surfaces quickly chill to black (<750 K [Kilburn, 1993]) and that water that comes in contact with these same black surfaces will typically flash to steam for several hours to days after emplacement (>373 K).

Our modeling approach is a simplified one which assumes a constant surface temperature from 100 s through the first ten hours of cooling. Fink and Griffiths [1992b] included heat loss

**Table 1.** Parameters for Crustal Growth Models

Parameter	Description	Value	Reference <sup>a</sup>
$k$	thermal diffusivity	$6 \times 10^{-7} \text{ m}^2 \text{ s}^{-1}$ basalt $7.5 \times 10^{-7} \text{ m}^2 \text{ s}^{-1}$ rhyolite	1, 2 1, 2
$L$	latent heat of crystallization	$4.2 \times 10^5 \text{ J kg}^{-1}$ basalt $2.9 \times 10^5 \text{ J kg}^{-1}$ rhyolite	1, 3 1, 3
$c$	specific heat	$1200 \text{ J kg}^{-1} \text{ K}^{-1}$ basalt	1, 4, 5
$T_e$	eruption temperature	1073 K rhyolite	6
$T_s$	solidus temperature	1373 K basalt	4
$T_g$	glass transition temperature	943 K rhyolite	7
$T_a$	ambient temperature	290 K Earth 750 K Venus	1, 8 1, 8

<sup>a</sup> 1, Bridges [1997]; 2, Peck et al. [1977]; 3, Huppert and Sparks [1988]; 4, Griffiths and Fink [1992a]; 5, Robertson [1988]; 6, Williams and McBirney [1979]; 7, Westrich et al. [1988]; 8, Griffiths and Fink [1992b].

by radiation and convection through 1000 seconds but included no latent heat release. They showed more than 500° of cooling for basaltic lava flows surfaces on both Earth and Venus in this time period, though <100° of this occurs after the first 100 s, during which the upper surface is quenched. As described above, *Bridges* [1997] considered radiative and convective losses through 1000 s and then made the assumption of a constant surface temperature after 10,000 s. We examine the propagation of selected isotherms into a flow to determine whether deformable crusts (>12 cm) form rapidly on Venusian flows during emplacement. Such a crust, if fractured and preserved at the surface, would be detectable in Magellan (12.6-cm wavelength) radar images. While the constant surface temperature assumption is an approximation, it allows inclusion of latent heat and provides a conservative approach. If the surface temperature were allowed to change throughout the first 10 hours of cooling, it would decrease and thus cause faster growth of the crust. For basaltic flows, inclusion of latent heat at times >100 s and use of the solidus isotherm to define the brittle crust also provide conservative estimates for crustal thickness at a given time.

For basaltic flows we have modeled the growth of the crust using the following expressions:

$$z = 2\lambda\sqrt{\kappa t} \quad (1)$$

[after Equation (4-129) *Turcotte and Schubert*, 1982] and

$$\frac{e^{-\lambda^2}}{\lambda \operatorname{erf} \lambda} = \frac{L\sqrt{\pi}}{c(T_s - T_0)} \quad (2)$$

[after Equation (4-134) *Turcotte and Schubert*, 1982] where  $z$  is thickness of surface crust,  $\lambda$  is the value of similarity variable at solidification boundary,  $k$  is thermal diffusivity,  $t$  is time,  $L$  is latent heat of crystallization,  $c$  is specific heat,  $T_s$  is solidus temperature, and  $T_0$  is temperature of the flow surface (which equals the ambient temperature  $T_a + 100$  K) [*Turcotte and Schubert*, 1982; *Bridges*, 1997]. The value of  $\lambda$  used to calculate the thickness of the crust can be found either iteratively or graphically using (2). Table 1 shows the relevant lava properties and boundary conditions. This solution results from using a similarity approach to solve the one-dimensional, time-dependent heat conduction equation with a thickening solid layer and heat released through crystallization [*Turcotte and Schubert*, 1982]. It assumes that both the upper surface of the crust and the liquid flow interior below the thickening crust are maintained at constant temperatures and is thus most appropriate for initial stages of crustal growth. This type of solution has been used to accurately model the solidification of Hawaiian lava lakes [*Wright et al.*, 1976; *Turcotte and Schubert*, 1982].

For rhyolitic flows, release of latent heat due to crystallization is not included. Solution of the heat conduction equation for cooling of a semi-infinite half-space initially of uniform temperature (equivalent to the eruption temperature  $T_e$ ) gives the following expression:

$$\frac{T - T_e}{T_0 - T_e} = \operatorname{erfc} \left[ \frac{z}{2\sqrt{\kappa t}} \right] \quad (3)$$

[after Equation (4-113) *Turcotte and Schubert*, 1982] where  $T$  can be assumed to be equivalent to the glass transition temperature  $T_g$  in order to solve for the position of the brittle-ductile transition as

a function of time. See Table 1 for model parameters. This approach also assumes that the surface temperature remains at a constant value.

### 3.3. Constraints From Models of Crustal Growth

We calculated the thickness of the brittle crust as a function of time as defined by the solidus temperature for basalt and the glass transition temperature for rhyolite (Figures 4a and 4b, respectively). These graphs show that brittle crusts of appreciable thickness (>10 cm) form within the first day for both basalts and rhyolites on Venus and that Venusian crusts are thinner than those on comparable terrestrial flows owing to the higher surface temperature on Venus. The progression of curves is in agreement with *Bridges* [1997] results after ~1 hour. As expected, comparison of our results with those of *Bridges*'s [1997] shows comparable but slightly thinner crusts for basaltic flows on Venus after 10,000 s; because of the different approaches used for rhyolite, our values for crustal thickness are noticeably smaller than those of *Bridges* [1997] after 10,000 s (~7 cm versus ~40 cm). In terms of understanding the deformation of lava flow surfaces on Venus and in particular the emplacement history of steep-sided domes, the model results indicate that brittle surface crusts >12 cm thick form within hours after flow emplacement for both basaltic (3.1 hours) and rhyolitic (8.3 hours) compositions. Therefore, if dome surfaces are subjected to the necessary stresses, brittle deformation should occur during transport. If the resulting surface features and blocks are preserved on dome surfaces, corresponding high radar backscatter signatures would be apparent in Magellan images [e.g. *J.J. Plaut et al.*, manuscript in preparation, 2000].

Recently, *Bullock and Grinspoon* [1996, 1998, submitted manuscript, 2000] have predicted that Venus may have experienced episodes of much higher surface temperatures (800–1000 K) in the past, caused by an intensified greenhouse brought on by large-scale volcanic resurfacing [e.g., *Schaber et al.*, 1992]. Higher surface temperatures would affect the spacing of tectonic features [*Solomon et al.*, 1998; *Phillips and Hansen*, 1998]. In addition, possible increases in surface temperature should influence the emplacement of volcanic flows. To assess the potential effects of these different ambient conditions, we used surface temperatures of 800 and 1000 K as ambient for basalt (Figure 4a). The glass transition temperature for rhyolite that we have used is 943 K, which is in the range of temperatures predicted in the hot Venus model. Therefore we modeled rhyolite crust formation at 842 K; hotter temperatures would result in a flow that does not quench. Figure 4b. illustrates that crust formation on a rhyolite flow is very sensitive to how close the ambient temperature is to the solidus temperature; a crust forms at 800 K, but very little crust forms at 842 K. Thus the only way to create a crust on a rhyolite flow in the hotter Venus case would be to allow the flow to cool slowly through its solidus (Figure 4c). For basalt, crusts still form relatively rapidly, despite the much hotter surface temperatures.

## 4. Discussion

### 4.1. A Model for Steep-Sided Dome Emplacement on Venus

Magellan radar backscatter data, surface morphology analysis, and crustal modeling provide constraints for a new model of Venus steep-sided dome formation. Our modeling (and that of *Bridges* [1997] and others) and the presence of pits on dome

surfaces are consistent with a crust being produced on eruptive timescales. The relatively smooth surfaces of the domes and dome fracture patterns indicate that surface crusts have not been broken into blocks, nor is any evidence of flow preserved. Our observations and modeling require a model for dome growth in which the brittle crust of the dome remains smooth and relatively

unfractured until late in its emplacement. We envision that as the dome is emplaced, the crust is continually pulled apart by tension as the flow moves outward from the vent (Figure 5). However, the timescales of crustal healing are sufficient that the crust is being continually annealed, resulting in a relatively smooth final surface [Kilburn, 1993; Kilburn and Lopes, 1991]. This is endogenous growth, where a continually healing crust permits the dome to grow by internal inflation [e.g., Griffiths and Fink, 1992b; Fink, 1993]. The large size and circular shape of the domes also make it difficult to maintain a stable crust, as new interior is continually exposed as material flows out radially from the vent. Surface features on the Venusian domes are consistent with this model. Fracture patterns and pits on the dome surfaces require a mobile interior, in agreement with endogenous growth. Surface strain rates were never high enough to produce blocks, or if they were, they resulted in entrainment and rehealing of the crust. This process is similar to that seen on terrestrial lava lakes [e.g., Macdonald, 1962]. Ridges (folds) do not form on the Venusian domes, as they would not develop a consistent vertical viscosity profile over a large area as required for folding to occur [e.g., Fink, 1980b].

In order to form the large diameters and circularity of Venusian domes, we require an initial core-dominated emplacement regime [Kilburn, 1993] where the crust does not appear to offer significant resistance to flow. Eventually, the core-dominated regime is replaced by a crust-dominated regime, which, coupled with diminished supply, would cause a dome to cease spreading. Variations in dome heights (thickness) may reflect differing amounts of endogenous growth beneath a stable crust. Very low slopes on Venus are also likely to contribute to dome circularity and also may help to explain why this annealing process may be more prevalent on Venus than Earth.

Alternatively, the morphology of steep-sided dome surfaces could be explained by formation of a brittle crust early in emplacement, followed by fracturing and block formation as the crust is deformed during dome growth, and then resurfacing of

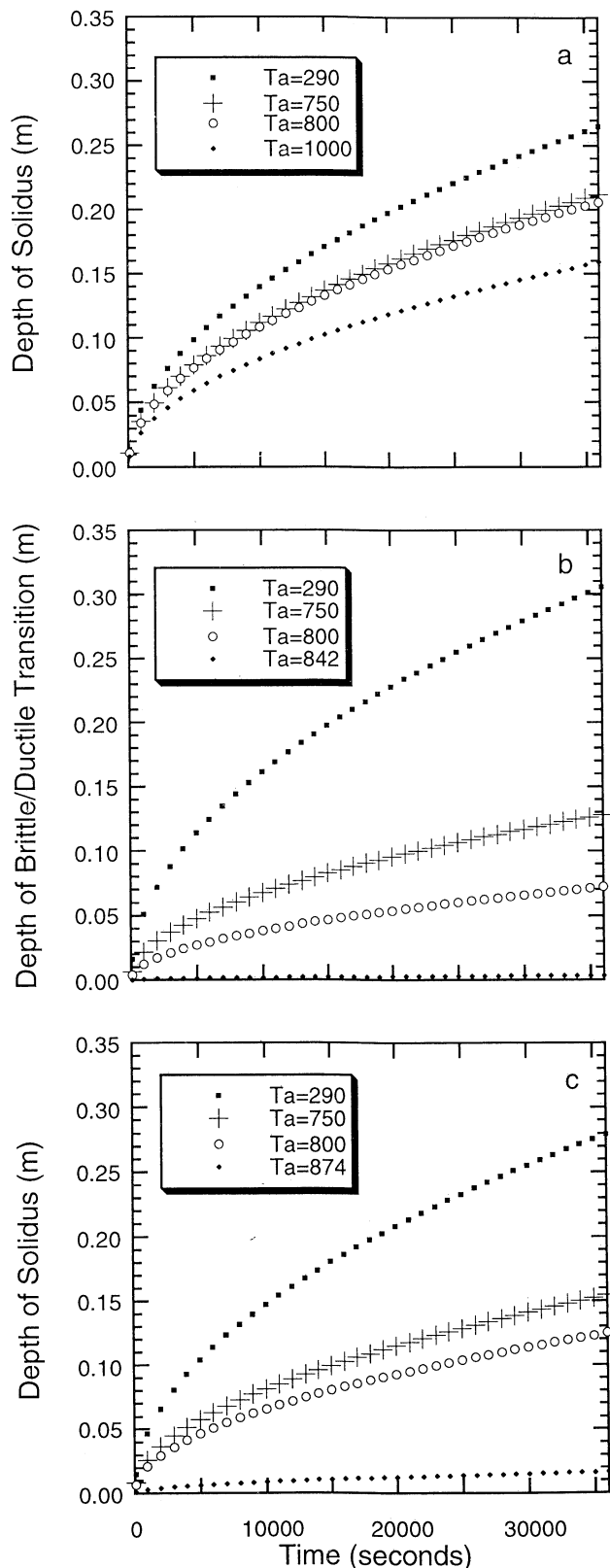
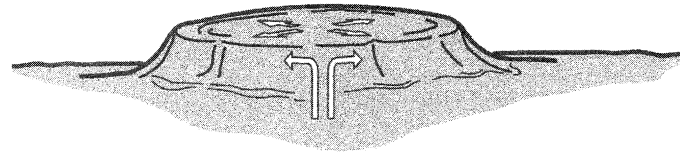
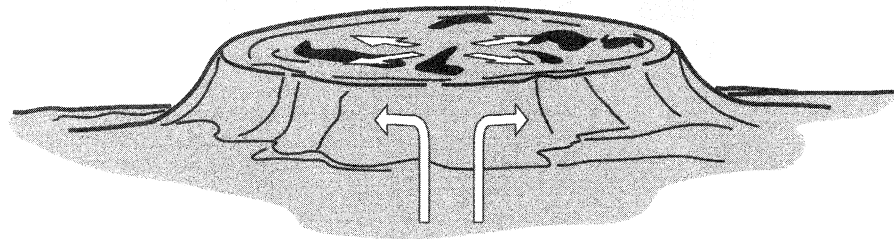


**Figure 4.** Growth rates for lava flow crust from times going from 100 s to 10 hours. (a) Crustal growth rates for basalt. Thickness of the crust is represented by the position of the solidus isotherm. Curves for current ambient temperatures of Earth (290 K) and Venus (750 K) as well as temperatures corresponding to the hotter Venus case (800-1000 K) are shown. A 12-cm crust forms on a terrestrial basalt flow in  $\sim 7000$  s (1.9 hours) and on a Venusian basalt flow in  $\sim 12,000$  s (3 hours). For the hotter Venus case, at 1000 K a 12-cm crust takes longer ( $\sim 20,000$  s or 5.6 hours) to form but still occurs within the first 10 hours. (b) Crustal growth rates for rhyolite. Thickness of the crust is represented by the position of the glass transition temperature isotherm. For current ambient conditions a 12-cm crust forms on Venus in  $\sim 5000$  s (1.4 hours). For temperatures within the range for a hotter Venus, a 12-cm crust is not produced within the first 10 hours; at 842 K, crustal thickness is  $< 1$  cm. (Note: owing to our assumption that the surface temperature is 100 K above ambient within the first 10 hours, the maximum temperature used in the modeling is limited to 100 K below the glass transition temperature.) (c) Crustal growth rates for rhyolite with thickness of the crust represented by the position of the solidus isotherm. For the hotter Venus case with latent heat released, crustal growth is still quite limited. At 874 K (100 K below the solidus), crustal growth is  $< 2$  cm after 10 hours. The possibility that the flow surface could remain above the solidus with high ambient temperatures indicates that a quenched crust would not form on a rhyolite flow even over long time periods.

### 1. Radial flow emplacement



### 2. Dome grows and thickens, crust continually healing



### 3. Dome cools, surface fracturing and pit formation

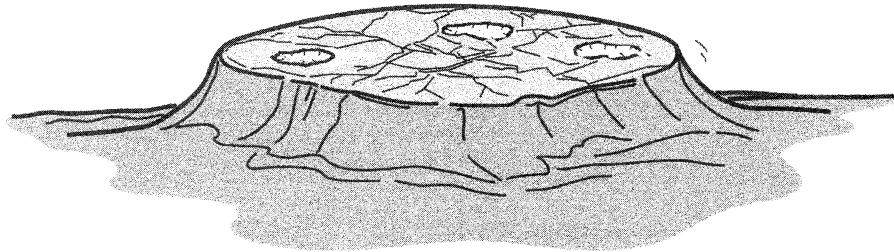


**Figure 5.** Schematic representation of dome growth. In the first stage the dome is emplaced on the surface, and a crust forms. In the second stage the crust cracks, is entrained, and heals as the dome thickens and grows. In the final cooling stages, the dome interior is still mobile, pits form, and the surface fractures as the dome cools.

the upper surface in the final stages of development. This dome-wide resurfacing stage would mask small fractures and potential blocky surfaces between larger fractures, resulting in the radar-smooth surfaces observed in the Magellan data. We do not favor this model owing to the unlikelihood of domes being completely resurfaced either by pyroclastic materials or lava, and the fact that no examples of partial dome resurfacing have been identified.

#### 4.2. Composition of Venusian Steep-Sided Domes

As stated above, previous studies have shown that compositional determinations based on gross morphology are nonunique [e.g., Sakimoto and Zuber, 1993, 1995], and parameters other than composition can control flow morphology [e.g., Fink and Griffiths, 1990; Bridges and Fink, 1992]. Our approach of analysis of surface features combined with modeling of crust formation, however, has provided some new constraints on dome composition. Entrainment and annealing of broken crust during emplacement, and polygonal fracturing generated by sagging both favor a low viscosity fluid. Thus we suspect that steep-sided domes on Venus are basaltic in composition. A basaltic composition is also favored by evidence that the core of the dome remained mobile for some time and had a low viscosity

and yield strength, as suggested by the polygonal fractures and collapse pits.

If the domes are silicic, under current Venus ambient conditions we would expect a crust to form and break into blocks, as at terrestrial domes and on the basis of our modeling of the formation of crusts. A thick rhyolitic or dacitic crust would be much less likely to allow crustal rehealing/annealing, as required in our model of Venusian dome growth, because of the high viscosity of the annealing material. For silicic domes we would expect convex dome profiles from accumulation of lava in the center of the dome as it is more difficult for high-viscosity lavas to flow away from the vent. Two Venusian domes have distinct upraised vent regions, and a small number of domes have rougher surfaces. While we suggest that the majority of steep-sided domes are likely basaltic in composition, some silicic domes may be present on Venus, especially those domes that are rough or have distinct, upraised vent regions.

Other than general gross characteristics (circularity, steep sides), our recent detailed observations do not directly support comparisons previously made between venusian domes and terrestrial rhyolite and dacite domes [e.g., Head et al., 1992; Pavri et al., 1992; Fink et al., 1993]. Terrestrial silicic domes have mappable surface morphologies, including vent regions,

jumbled regions, and ridged areas, although the areal extent of the various units may vary between domes [Anderson *et al.*, 1998]. Similar mappable surface morphologies and structures have not been identified in the Magellan images of Venusian steep-sided domes. In addition, catastrophic failure of dome margins and interiors appears to be common on Venus [Guest *et al.*, 1992; Bulmer and Guest, 1996] but is not typical on Earth at silicic domes except in regions of steep slopes (e.g., Unzen) [Nakada and Fujii, 1993; Nakada *et al.*, 1995].

Alternatively, if Venus underwent a time period in which the surface temperatures increased to 800-1000 K, as suggested by Bullock and Grinspoon [1996, 1998, submitted manuscript, 2000], our model indicates that a glassy crust would form on a rhyolite flow. Therefore, under the hot Venus scenario, dome characteristics are consistent with either basaltic or rhyolitic compositions.

## 5. Conclusions

Steep-sided domes on Venus exhibit surface features that provide information on their origin and emplacement. Radar backscatter data of the domes indicate that they have smooth, relatively unbroken surfaces. Radial fracture patterns seen at some domes are consistent with endogenous growth, while polygonally fractured domes reflect sagging and cooling. Pits on dome surfaces are consistent with a fluid interior under cooling carapace, with limited evidence of secondary explosive activity. Pit depths provide a minimum crustal thickness estimate of tens of meters. This surface evidence suggests that the Venusian steep-sided domes did not form a stable brittle crust until the final stages of their emplacement.

We have calculated the time necessary to form a 12-cm-thick crust for basalt and rhyolite under terrestrial and Venusian ambient conditions. This crustal thickness is the minimum necessary to form a surface block with dimensions similar to that of the Magellan radar wavelength (12.6 cm). The differences between the times necessary to form a 12-cm crust under these conditions is less than an order magnitude, with subaerial rhyolite forming a crust most rapidly (<2 hours), followed by subaerial basalt, Venusian basalt, and Venusian rhyolite (~8 hours). A 12-cm brittle crust will form on all compositions in <10 hours under ambient Venusian and terrestrial conditions. Thus Venusian lava flows should develop a brittle carapace during emplacement.

Constraints from evaluation of surface morphology and results of thermal modeling clearly narrow the range of viable emplacement models for steep-sided Venusian domes. Thermal modeling shows that brittle surface crusts form rapidly on Venus, yet only the late-stage brittle fractures are preserved. Thus the early-formed surface crust must be resurfaced, entrained, or continually annealed as it deforms to accommodate dome growth. Resurfacing must completely cover all of the domes in our survey in order to completely erase all evidence of early crust formation and is therefore unlikely. Entrainment and annealing of fractures are not mutually exclusive processes and thus may both be at work during steep-sided dome emplacement. This process is similar to that seen at terrestrial lava lakes and may be more prevalent on Venus owing to the low slopes of the Venusian plains.

Our results are most consistent with basaltic compositions, as rhyolitic lavas would quickly form thick crusts which would break into large blocks that would be difficult to entrain or anneal. Under the hotter Venus scenario suggested by Bullock

and Grinspoon [1998, submitted manuscript, 2000], rhyolitic lavas would be unable to form crusts, and therefore steep-sided dome characteristics would be consistent with either basaltic or rhyolitic compositions.

**Acknowledgments.** The authors would like to acknowledge helpful discussions with John Guest, Mark Bulmer and Tracy Gregg and assistance with compilation of the dome database from Jeff Byrnes, Kristen Fraga and Craig Nakan. The authors gratefully acknowledge the NASA/Venus Data Analysis Program grant which funded the initial stages of this work, as well as support to ERS from a Presidential Early Career Award (NASA).

## References

- Anderson, S.W., and J.H. Fink, Hydrogen isotope evidence for extrusion mechanisms of the Mount St. Helens dome, *Nature*, *341*, 521-523, 1989.
- Anderson, S.W., and J.H. Fink, The development and distribution of surface textures at the Mount St. Helens dome, in *Lava Flows and Domes: Emplacement Mechanisms and Hazard Implications*, edited by J.H. Fink, *IAVCEI Proc. Volcanol.*, *2*, 25-46, 1990.
- Anderson, S.W., and J.H. Fink, Crease structures: Indicators of emplacement rates and surface stress regimes of lava flows, *Geol. Soc. Am. Bull.*, *104*, 615-625, 1992.
- Anderson, S.W., D.A. Crown, J.J. Plaut, and E.R. Stofan, Surface characteristics of steep-sided domes on Venus and terrestrial silicic domes: A comparison, *Lunar Planet. Sci.*, *XXV*, 33-34, 1994.
- Anderson, S.W., J.H. Fink, and W.I. Rose, Mount St. Helens and Santiaguito lava domes: The effect of short-term eruption rate on surface texture and degassing processes, *J. Volcanol. Geotherm. Res.*, *69*, 105-116, 1995.
- Anderson, S.W., E.R. Stofan, J.J. Plaut, and D.A. Crown, Block size distributions on silicic lava flow surfaces: Implications for emplacement conditions, *Geol. Soc. Am. Bull.*, *110*, 1258-1267, 1998.
- Anderson, S.W., E.R. Stofan, S.E. Smrekar, J.E. Guest, and B. Wood, Pulsed inflation of pahoehoe lava flows: Implications for flood basalt emplacement, *Earth Planet. Sci. Lett.*, *168*, 7-18, 1999.
- Aydin, A., and J.M. DeGraff, Evolution of polygonal fracture patterns in lava flows, *Science*, *239*, 471-476, 1988.
- Blake, S., Viscoplastic models of lavas domes, in *Lava Flows and Domes: Emplacement Mechanisms and Hazard Implications*, edited by J.H. Fink, *IAVCEI Proc. Volcanol.*, *2*, 88-126, 1990.
- Bridges, N.T., Submarine analogs to Venusian pancake domes, *Geophys. Res. Lett.*, *22*, 2781-2784, 1995.
- Bridges, N.T., Ambient effects on basalt and rhyolite lavas under Venusian, subaerial, and subaqueous conditions, *J. Geophys. Res.*, *102*, 9243-9255, 1997.
- Bridges, N.T., and J.H. Fink, Aspect ratios of lava domes on Earth, Moon and Venus, *Lunar Planet. Sci.*, *XXIII*, 159-160, 1992.
- Bullock, M.A., and D.H. Grinspoon, The stability of climate on Venus, *J. Geophys. Res.*, *101*, 7521-7529, 1996.
- Bullock, M.A., and D.H. Grinspoon, Geological forcing of surface temperatures on Venus, *Lunar Planet. Sci.*, *XXIX* [CD-ROM], abstract 1542, 1998.
- Bulmer, M.H., and J.E. Guest, Modified volcanic domes and associated debris aprons on Venus, in *Volcano Instability*, edited by W.J. McGuire, A.P. Jones, and J. Neuberger, *Geol. Soc. Spec. Publ.*, *110*, 349-371, 1996.
- Campbell, B.A., and M.K. Shephard, Lava flow surface roughness and depolarized radar scattering, *J. Geophys. Res.*, *101*, 18,941-18,951, 1996.
- Cashman, K.V., Textural constraints on the kinetics of crystallization of igneous rocks, *Rev. Mineral.*, *24*, 259-314, 1990.
- Cashman, K.V., Groundmass crystallization of Mount St. Helens dacite, 1980-1986: A tool for interpreting shallow magmatic processes, *Contrib. Mineral. Petrol.*, *109*, 431-449, 1992.
- Cashman, K.V., Relationship between crystallization and cooling rate -- Insight from textural studies of dikes, *Contrib. Mineral. Petrol.*, *113*, 126-142, 1993.
- Cashman, K.V., and J.E. Taggart, Petrologic monitoring of 1981 and 1982 eruptive products from Mount St. Helens, *Science*, *221*, 1385-1387, 1981.
- Cashman, K.V., C. Thornber, and J.P. Kauahikaua, Cooling and crystallization of lava in open channels, and the transition of pahoehoe lava to aa, *Bull. Volcanol.*, *61*, 306-323, 1999.

- Crisp, J.A., and S.M. Baloga, A model for lava flows with two thermal components, *J. Geophys. Res.*, **95**, 1255-1270, 1990.
- Crisp, J.A., and S.M. Baloga, Influence of crystallization and entrainment of cooler material on the emplacement of basaltic aa lava flows, *J. Geophys. Res.*, **99**, 11,819-11,831, 1994.
- Crisp, J., K.V. Cashman, J.A. Bonini, S.B. Hougén, and D.C. Pieri, Crystallization history of the 1984 Mauna Loa lava flow, *J. Geophys. Res.*, **99**, 7177-7198, 1994.
- Crown, D.A., E.R. Stofan, and J.J. Plaut, Volcanism in southern Guinevere Planitia, Venus: Regional volcanic history and morphology of volcanic domes, *Lunar Planet. Sci.*, **XXIV**, 355-356, 1993.
- DeGraff, J.M., and A. Aydin, Surface morphology of columnar joints and its significance to mechanics and direction of joint growth, *Geol. Soc. Am. Bull.*, **99**, 605-617, 1987.
- DeGraff, J.M., and A. Aydin, Effect of thermal regime on growth increment and spacing of contraction joints in basaltic lava, *J. Geophys. Res.*, **98**, 6411-6430, 1993.
- de Silva, S.L., S. Self, and P.W. Francis, The Chao dacite revisited, *Eos Trans. AGU*, **69**, 1491, 1988.
- Fink, J.H., Gravity instability in the Holocene Big and Little Glass Mountain rhyolitic obsidian flows, northern California, *Tectonophysics*, **66**, 147-166, 1980a.
- Fink, J.H., Surface folding and viscosity of rhyolite flows, *Geology*, **8**, 250-254, 1980b.
- Fink, J.H., Structure and emplacement of a rhyolitic obsidian flow: Little Glass Mountain, Medicine Lake Highland, northern California, *Geol. Soc. Am. Bull.*, **94**, 362-380, 1983.
- Fink, J.H., Geometry of silicic dikes beneath the Inyo domes, California, *J. Geophys. Res.*, **90**, 11,127-11,133, 1985.
- Fink, J.H., The emplacement of silicic lava flows and associated hazards, in *Active Lavas*, edited by C.R.J. Kilburn and G. Luongo, pp. 5-24, Univ. College London Press, London, 1993.
- Fink, J.H., and R.C. Fletcher, Ropy pahoehoe: Surface folding of a viscous fluid, *J. Volcanol. Geotherm. Res.*, **4**, 151-170, 1978.
- Fink, J.H., and R.W. Griffiths, Radial spreading of viscous-gravity currents with solidifying crust, *J. Fluid Mech.*, **221**, 485-509, 1990.
- Fink, J.H., and C.R. Manley, Origin of pumiceous and glassy textures in rhyolite flows and domes, in *The Emplacement of Silicic Domes and Lava Flows*, edited by J.H. Fink, *Spec. Pap. Geol. Soc. Am.*, **212**, 77-88, 1987.
- Fink, J.H., and D.D. Pollard, Structural evidence for dikes beneath silicic domes, Medicine Lake Highland, California, *Geology*, **11**, 458-461, 1983.
- Fink, J.H., S.W. Anderson, and C.R. Manley, Textural constraints on effusive silicic volcanism: Beyond the permeable foam model, *J. Geophys. Res.*, **97**, 9073-9083, 1992.
- Fink, J.H., N.T. Bridges, and R.E. Grimm, Shapes of Venusian "pancake" domes imply episodic emplacement and silicic composition, *Geophys. Res. Lett.*, **20**, 261-264, 1993.
- Ford, P.G., Radar scattering properties of steep-sided domes on Venus, *Icarus*, **112**, 204-218, 1994.
- Ford, P.G., and G.H. Pettengill, Venus topography and kilometer-scale slopes, *J. Geophys. Res.*, **97**, 13,103-13,114, 1992.
- Gregg, T.K.P., and R. Greeley, Formation of Venus canali: Considerations of lava types and their thermal behaviors, *J. Geophys. Res.*, **98**, 10,873-10,882, 1993.
- Gregg, T.K.P., and S.E.H. Sakimoto, Venusian lava flow morphologies: Variations on a basaltic theme, *Lunar Planet. Sci.*, **XXVII**, 459-460, 1996.
- Gregg, T.K.P., J.H. Fink, and R.W. Griffiths, Formation of multiple fold generations on lava flow surfaces: Influence of strain rate, cooling rate, and lava composition, *J. Volcanol. Geotherm. Res.*, **80**, 281-292, 1998.
- Griffiths, R.W., and J.H. Fink, Solidification and morphology of submarine lavas: A dependence on extrusion rate, *J. Geophys. Res.*, **97**, 19,729-19,738, 1992a.
- Griffiths, R.W., and J.H. Fink, The morphology of lava flows in planetary environments: Predictions from analog experiments, *J. Geophys. Res.*, **97**, 19,739-19,748, 1992b.
- Guest, J.E., and J. Sanchez, A large dacitic lava flow in northern Chile, *Bull. Volcanol.*, **33**, 778-790, 1969.
- Guest, J.E., M.H. Bulmer, J. Aubele, K. Beratan, R. Greeley, J.W. Head, G. Michaels, C. Weitz, and C. Wiles, Small volcanic edifices and volcanism in the plains of Venus, *J. Geophys. Res.*, **97**, 15,949-15,966, 1992.
- Head, J.W., and L. Wilson, Volcanic processes and landforms on Venus: Theory, predictions, and observations, *J. Geophys. Res.*, **91**, 9407-9446, 1986.
- Head, J.W., D.B. Campbell, C. Elachi, J.E. Guest, D.P. McKenzie, R.S. Saunders, G.G. Schaber, and G. Schubert, Venus volcanism: Initial analysis from Magellan data, *Science*, **252**, 276-288, 1991.
- Head, J.W., L.S. Crumpler, J.C. Aubele, J.E. Guest, and R.S. Saunders, Venus volcanism: Classifications of volcanic features and structures, associations, and global distribution from Magellan data, *J. Geophys. Res.*, **97**, 13,153-13,198, 1992.
- Huppert, H.E., and R.S.J. Sparks, The generation of granitic magmas by intrusion of basalt into continental crust, *J. Petrol.*, **29**, 599-624, 1988.
- Iverson, R.M., Lava domes modeled as brittle shells that enclose pressurized magma, with application to Mount St. Helens, in *Lava Flows and Domes: Emplacement Mechanisms and Hazard Implications*, edited by J.H. Fink, *IAVCEI Proc. Volcanol.*, **2**, 47-69, 1990.
- Johnson, C.L., and D.T. Sandwell, Joints in Venusian lava flows, *J. Geophys. Res.*, **97**, 13,601-13,610, 1992.
- Johnson, R.B., Patterns and the origin of radial dike swarms associated with West Peak and Dike Mountain, south-central Colorado, *Geol. Soc. Am. Bull.*, **72**, 579-590, 1961.
- Johnson, R.B., Geology of the igneous rocks of the Spanish Peaks region, Colorado, *U.S. Geol. Surv. Prof. Pap.*, **594-G**, 1968.
- Kilburn, C.R.J., Lava crusts, aa flow lengthening and the pahoehoe-aa transition, in *Active Lavas*, edited by C.R.J. Kilburn and G. Luongo, pp. 263-280, Univ. College London Press, London, 1993.
- Kilburn, C.R.J., and R.M.C. Lopes, General patterns of flow field growth: Aa and blocky lavas, *J. Geophys. Res.*, **96**, 19,721-19,732, 1991.
- Loney, R.A., Flow structure and composition of the Southern Coulee, Mono Craters, California: A pumiceous rhyolite flow, in *Studies in Volcanology*, edited by R.R. Coats, R.L. Hay, and C. Anderson, *Mem. Geol. Soc. Am.*, **116**, 415-440, 1968.
- Long, P.E., and B.J. Wood, Structures, textures and cooling histories of Columbia River basalt flows, *Geol. Soc. Am. Bull.*, **97**, 1144-1155, 1986.
- Macdonald, G.A., The 1959 and 1960 eruptions of Kilauea Volcano, Hawaii and the construction of walls to restrict the spread of the lava flows, *Bull. Volcanol.*, **24**, 249-294, 1962.
- Manley, C.R., and J.H. Fink, Internal textures of rhyolite flows as revealed by research drilling, *Geology*, **15**, 549-552, 1987.
- McKenzie, D., P.G. Ford, F. Liu, and G.H. Pettengill, Pancake-like domes on Venus, *J. Geophys. Res.*, **97**, 15,967-15,976, 1992.
- Moore, H.J., J.J. Plaut, P.M. Schenk, and J.W. Head, An unusual volcano on Venus, *J. Geophys. Res.*, **97**, 13,479-13,494, 1992.
- Moore, J.G., P.W. Lipman, D.A. Swanson, and T.R. Alpha, Growth of lava domes in the crater, June 1980-January 1981, in *The 1980 Eruptions of Mount St. Helens, Washington*, edited by P.W. Lipman and D.R. Mullineaux, *U.S. Geol. Surv. Prof. Pap.*, **1250**, 541-548, 1981.
- Murase, T., and A.R. McBirney, Viscosity of lunar lavas, *Science*, **167**, 1491-1493, 1970.
- Nakada, S., and T. Fujii, Preliminary report on volcanic activity at Unzen Volcano, November 1990-November 1991: Dacite lava domes and pyroclastic flows, *J. Volcanol. Geotherm. Res.*, **54**, 319-333, 1993.
- Nakada, S., Y. Miyake, H. Sato, O. Oshima, and A. Fujinawa, Endogenous growth of dacite dome at Unzen volcano (Japan), 1993-1994, *Geology*, **23**, 157-160, 1995.
- Neuville, D.R., P. Courtial, D.B. Dingwell, and P. Richet, Thermodynamic and rheological properties of rhyolite and andesite melts, *Contrib. Mineral. Petrol.*, **113**, 572-581, 1993.
- Nichols, R.L., Viscosity of lava, *J. Geol.*, **47**, 290-302, 1939.
- Pavri, B., J.W. Head, K.B. Klose, and L. Wilson, Steep-sided domes on Venus: Characteristics, geologic setting, and eruption conditions from Magellan data, *J. Geophys. Res.*, **97**, 13,445-13,478, 1992.
- Peck, D.L., M.S. Hamilton, and H.R. Shaw, Numerical analysis of lava lake cooling models, 2, Application to Alae lava lake, Hawaii, *Am. J. Sci.*, **277**, 415-437, 1977.
- Phillips, R.J., and V.L. Hansen, Geological evolution of Venus: Rises, plains, plumes and plateaus, *Science*, **279**, 1492-1497, 1998.
- Plaut, J.J., Stereo imaging, in *Guide to Magellan Image Interpretation*, *JPL Pub.*, **93-24**, 33-44, 1993.
- Plaut, J.J., E.R. Stofan, D.A. Crown, and S.W. Anderson, Steep-sided volcanic domes on Venus and Earth: Macro-scale geometry from remote sensing and field measurements, *Eos Trans. AGU*, **74(43)**, Fall Meet. Suppl., 379, 1993.
- Plaut, J.J., E.R. Stofan, D.A. Crown, and S.W. Anderson, Topographic

- and surface roughness properties of steep-sided domes on Venus and Earth from radar remote sensing and field measurements, *Lunar Planet. Sci.*, XXV, 1091-1092, 1994.
- Reches, Z., and J. Fink, The mechanism of intrusion of the Inyo Dikes, Long Valley Caldera, California, *J. Geophys. Res.*, 93, 4321-4334, 1988.
- Robertson, E.C., Thermal properties of rocks, *U.S. Geol. Surv. Open File Rep.*, 88-441, 106 pp., 1988.
- Rossi, M.J., and A. Gudmundsson, The morphology and formation of flow-lobe tumuli on Icelandic shield volcanoes, *J. Volcanol. Geotherm. Res.*, 72, 291-308, 1996.
- Ryan, M.P., and C.G. Sammis, Cyclic fracture mechanisms in cooling basalt, *Geol. Soc. Am. Bull.*, 89, 1295-1308, 1978.
- Ryan, M.P., and C.G. Sammis, The glass transition in basalt, *J. Geophys. Res.*, 86, 9519-9535, 1981.
- Sakimoto, S.E.H., and M.T. Zuber, Venus pancake dome formation: Morphologic effects of a cooling-induced variable viscosity during emplacement, *Lunar Planet. Sci.*, XXIV, 1233-1234, 1993.
- Sakimoto, S.E.H., and M.T. Zuber, The spreading of variable-viscosity axisymmetric radial gravity currents: Applications to the emplacement of Venusian 'pancake' domes, *J. Fluid Mech.*, 301, 65-77, 1995.
- Sampson, D.E., Textural heterogeneities and vent area structures in the 600-year-old lavas of the Inyo volcanic chain, eastern California, in *The Emplacement of Silicic Domes and Lava Flows*, edited by J.H. Fink, *Spec. Pap. Geol. Soc. Am.*, 212, 89-101, 1987.
- Saunders, R.S., R. Arvidson, J.W. Head, G.G. Schaber, S.C. Solomon, and E.R. Stofan, Magellan: A first overview of Venus geology, *Science*, 252, 249-252, 1991.
- Saunders, R.S., et al., Magellan mission summary, *J. Geophys. Res.*, 97, 13,067-13,090, 1992.
- Schaber, G.G., H.J. Moore, R.G. Strom, L.A. Soderblom, L.R. Gaddis, J.M. Boyce, R.L. Kirk, D.J. Chadwick, and J. Russell, The geology and distribution of impact craters on Venus: What are they telling us?, *J. Geophys. Res.*, 97, 13,257-13,302, 1992.
- Scott, W.E., Holocene rhyodacite eruptions on the flanks of South Sister volcano, Oregon, in *The Emplacement of Silicic Domes and Lava Flows*, edited by J.H. Fink, *Spec. Pap. Geol. Soc. Am.*, 212, 35-54, 1987.
- Smith, E.I., Mono Craters, California: A new interpretation of the eruptive sequence, *Geol. Soc. Amer. Bull.*, 84, 2685-2690, 1973.
- Solomon, S.C., M.A. Bullock and D.H. Grinspoon, Climate change as a regulator of global tectonics on Venus, *Lunar and Planetary Sci.* XXIX, 1624, 1998.
- Spry, A., The origin of columnar jointing, particularly in basalt flows, *Geol. Soc. Aust. J.*, 8, 191-216, 1962.
- Stevenson, R.J., D.B. Dingwell, S.L. Webb, and T.L. Sharp, Viscosity of microlite-bearing rhyolitic obsidians: An experimental study, *Bull. Volcanol.*, 58, 298-309, 1996.
- Swanson, D.A., D. Dzurisin, R.T. Holcomb, E.Y. Iwatsubo, W.W. Chadwick, T.J. Casadevall, J.W. Ewert, and C.C. Heliker, Growth of the lava dome at Mount St. Helens, Washington (USA), 1981-1983, in *The Emplacement of Silicic Domes and Lava Flows*, edited by J.H. Fink, *Spec. Pap. Geol. Soc. Am.*, 212, 1-16, 1987.
- Turcotte, D.L., and G. Schubert, *Geodynamics*, 450 pp., John Wiley, New York, 1982.
- Walker, G.P.L., Three Hawaiian calderas: An origin through loading by shallow intrusions?, *J. Geophys. Res.*, 93, 14,773-14,784, 1988.
- Walker, G.P.L., Structure, and origin by injection of lava under surface crust, of tumuli, "lava rises", "lava-rise pits", and "lava-inflation clefts" in Hawaii, *Bull. Volcanol.*, 53, 546-558, 1991.
- Webb, S., Silicate melts: Relaxation, rheology and the glass transition, *Rev. Geophys.*, 35, 191-218, 1997.
- Westrich, H.R., H.W. Stockman, and J.C. Eichelberger, Degassing of rhyolitic magma during ascent and emplacement, *J. Geophys. Res.*, 93, 6503-6511, 1988.
- Williams, H., and A.R. McBirney, *Volcanology*, 397 pp., W. H. Freeman, New York, 1979.
- Wright, T.L., D.L. Peck, and H.R. Shaw, Kilauea lava lakes: Natural laboratories of study of cooling, crystallization and differentiation of basaltic magma, in *The Geophysics of the Pacific Ocean Basin and Its Margin*, *Geophys. Monogr. Ser.*, vol. 19, edited by G.H. Sinton, M.H. Manghnani, and R. Moberly, pp. 375-390, AGU, Washington, D. C., 1976.

S.W. Anderson, Black Hills State University, Spearfish, SD 57799.

D.A. Crown, Department of Geology and Planetary Science, University of Pittsburgh, Pittsburgh, PA 15260.

J.J. Plaut and E.R. Stofan, Jet Propulsion Laboratory, California Institute of Technology, 4800 Oak Grove Drive, Pasadena, CA 91109. (ellen.r.stofan@jpl.nasa.gov)

(Received, October 22, 1999; revised June, 27, 2000; accepted August 29, 2000)